

Many-body localization in a non-Hermitian quasi-periodic system

Liang-Jun Zhai¹, Shuai Yin², Guang-Yao Huang^{3*}

¹*The school of mathematics and physics, Jiangsu University of Technology, Changzhou 213001, China*

²*School of Physics, Sun Yat-Sen University, Guangzhou 510275, China and*

³*Institute for Quantum Information & State Key Laboratory of High Performance Computing, College of Computer, National University of Defense Technology, Changsha 410073, China*

(Dated: July 9, 2020)

In present study, the interplay among interaction, topology, quasi-periodicity, and non-Hermiticity is studied. The hard-core bosons model on a one-dimensional lattice with an asymmetry hopping and a quasi-periodic onsite potential is selected. This model, which preserves time-reversal symmetry, will exhibit three types of phase transitions: real-complex eigenenergies transition, topological phase transition and many-body localization phase transition. In the real-complex eigenenergies transition, it is found that the imaginary parts of the eigenenergies are always suppressed by the many-body localization. Moreover, by calculating the winding number, a topological phase transition can be revealed with the increase of potential amplitude, and we find that the behavior is quite different from the single-particle systems. Based on our numerical results, we conjecture that these three types of transition occur at the same point in the thermodynamic limit, and the many-body localization transition of quasi-periodic system and disorder system should belong to different universality class. Finally, we demonstrate that these phase transition can profoundly affect the dynamics of the non-Hermitian many-body system.

I. INTRODUCTION

In recent years, as an extension of the non-interacting Anderson localization, a phenomenon termed as many-body localization (MBL) in the quantum many-body systems has received a lot of attention^{1–14}. In such a phase, the system fails to act as a bath for its own subsystems and thermalization does not occur. It has been established that MBL phase has drastically different spectra and dynamical properties comparing with the delocalization (thermal) phase. Although MBL is usually studied for systems with random disorder, there is another type of system, the quasi-periodic system, also supports MBL due to its unique features^{15–31}. The quasi-periodic system breaks translational invariance by the incommensurate period, and shows some random-like properties similar to the disorder systems. However, comparing with disorder system, the quasi-periodic system has a long-range correlation, and introduce a disorder in a more controlled way. Thus the quasi-periodic systems constitute an intermediate phase between periodic system and fully disordered system. In the previous theoretical studies, it has been found that MBL phase transition in the hermitian disorder system and quasi-periodic system belongs to two distinct universality classes^{19,20}, and MBL phase in quasi-periodic systems is more stable as compared to the disorder systems²⁰.

Most recently, great interest has been devoted to study the MBL phenomena in the non-Hermitian systems^{32–36}. The results showed that many-body localization signatures can be restored even in the appearance of the dissipation³³. In some class non-Hermitian systems with time-reversal symmetry, there are real-complex transition of eigenenergies featuring parity-time (PT) symmetry^{37–40}. It is found that MBL can suppress the imaginary parts of the complex eigenenergies of disordered

systems, and the real-complex transition of eigenenergies occurs accompanied with the MBL phase transition³². On the other hand, exotic topological phases were unveiled in the non-Hermitian quantum systems^{41–50}. For the non-Hermitian single particle systems, theoretical studies found that the localization-delocalization transition for both the disorder and quasi-periodic systems has a topological nature, and the localization and delocalization phases can be characterized by the winding number^{45,46,49}. For the Hermitian many-body systems, it has been found that the interactions can destroy the topological phase or create new topological phase which are topologically distinct from the trivial states^{51–53}, and MBL eigenstates can exhibit or fail to exhibit topological orders^{54–57}. However, for the non-Hermitian many-body systems, there are seldom work has been done to investigate the affection of the interaction on the topological phase and the relations between the topological and MBL phase transition.

With this background, the interplay among interaction, topology, quasi-periodicity, and non-Hermiticity is explored in this paper. The study is applied to a hard-core bosons model on a one-dimensional lattice with an asymmetry hopping and a quasi-periodic onsite potential. The non-Hermiticity of the model comes from the asymmetry hopping, but it still has the time-reversal symmetry. We find that the MBL phase transition, real-complex eigenenergies transition and topological phase transition coexist for this model, and the transition points of these transition are close. The obtained critical exponent of quasi-periodic system is different from the disorder systems, which means the they belong to different universality class. Based on our numerical results, we conjecture that these three transitions occur at the same point in the thermodynamic limit. Since the real-complex eigenenergies transition and MBL phase

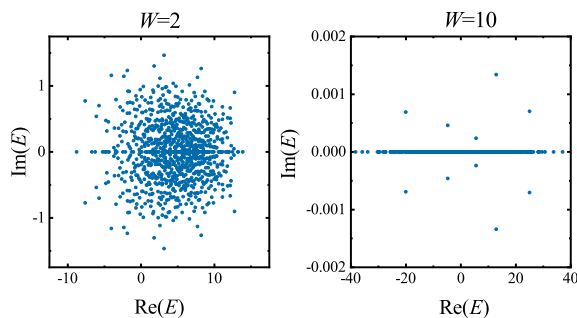


FIG. 1. Eigenenergies of the Hamiltonian Eq. (1) with $W = 2$ (left) and $W = 10$ (right). Here, the lattice size is $L = 12$.

transition can profoundly affect the dynamics of the non-Hermitian system⁵⁸, the dynamical behaviors of real part of eigenenergy and entanglement entropy are studied.

The remainder of the paper is organized as follows. In Section II, the model of the non-Hermitian quasi-periodic system is presented. Numerical investigation is presented in Section III. A summary is given in Section IV.

II. MODEL

A non-Hermitian hard-core bosons model on a one-dimensional lattice is considered in present study. The Hamiltonian reads

$$\hat{H} = \sum_{i=1}^L [-J(e^{-g}\hat{b}_{i+1}^\dagger\hat{b}_i + e^g\hat{b}_i^\dagger\hat{b}_{i+1}) + U\hat{n}_i\hat{n}_{i+1} + W_i\hat{n}_i] \quad (1)$$

Here, \hat{b}_i and \hat{b}_i^\dagger are the annihilation and creation operators of a hard-core boson, and $\hat{n}_i = \hat{b}_i^\dagger\hat{b}_i$ is the particle-number operator at site i . J and g label the asymmetry hopping amplitude between the nearest-neighboring (NN) sites, and U is the interaction between NN sites. For a quasi-periodic system, the onsite potential is $W_i = W \cos(2\pi\alpha i + \phi)$, where W is the amplitude of the potential, and ϕ is the phase of the potential, and α is irrational for incommensurate potentials.

For this model, the non-Hermiticity is controlled by the parameter g , but it still have the time-reversal symmetry. In the following, we assume $J = 1$, $U = 2$, $g = 0.5$, and the subspace with fixed particle number $M = L/2$ is selected. The irrational number α is chosen as the inverse of the golden mean $\alpha = (\sqrt{5} - 1)/2$, which could be compared with the experimental results¹⁶. The periodic boundary condition is assumed in the following calculation.

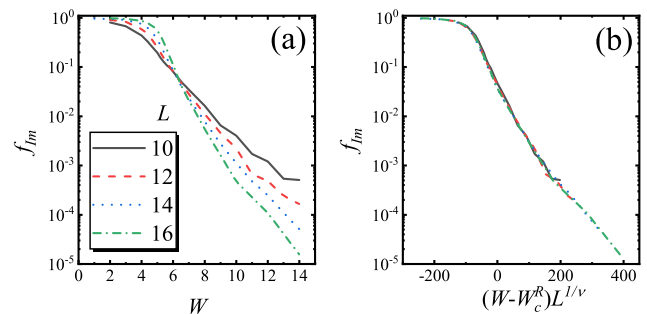


FIG. 2. (a) f_{Im} as a function of W for $L = 10, 12, 14$ and 16 , and (b) the rescaled curves according to Eq. (3).

III. NUMERICAL RESULTS AND DISCUSSIONS

A. Real-complex eigenenergies transition

Firstly, the real-complex eigenenergies transition of this model is studied. As shown in Fig. 1, the eigenenergies of Hamiltonian Eq. (1) with $L = 12$ and different W are plotted. Since the non-Hermitian Hamiltonian still have the time-reversal symmetry, it is found that the imaginary parts of the sperm is symmetric around the real axis. With the increase of W , the eigenenergies with nonzero imaginary parts decrease.

To measure the variation of the ratio of the complex eigenenergies with nonzero imaginary parts, f_{Im} is defined as

$$f_{Im} = \overline{D_{Im}/D}, \quad (2)$$

where the D_{Im} is the number of eigenenergies with nonzero imaginary part, and D is the total number of eigenenergies. Here, a cutoff of $C = 10^{-13}$ is used, that is, $|\text{Im}E| \leq C$ is identified to be a machine error. In Fig. 2(a), f_{Im} as a function of W for different L is plotted, and the results are obtained by averaging 500 choice of ϕ for $L = 10, 12$ and 14 , and 100 choice of ϕ for $L = 16$. Roughly speaking, when $W \leq W_C^R = 6.6$, f_{Im} increases with the increase of L , while f_{Im} decreases with the increase of L for $W \geq W_C^R$. The curves of f_{Im} as a function of W can be rescaled by the following scaling function

$$f_{Im} \propto (W - W_C^R)L^{1/\nu}, \quad (3)$$

where $\nu = 0.7$. As shown in Fig. 2(b), the rescaled curves collapse onto each other, which confirms Eq. (3). These results demonstrate that in the thermodynamic limit ($L \rightarrow \infty$) the model of Eq. (1) should have a complex-real phase transition at $W = W_C^R$, that is, when $W < W_C^R$ the eigenenergies is almost complex, while the eigenenergies are almost real for $W > W_C^R$. Similar result has also been found in the non-Hermitian Hamiltonian with a random onsite potential³², but the scaling exponent ν for the disorder system is different with we found here, which means the complex-real phase transition should be

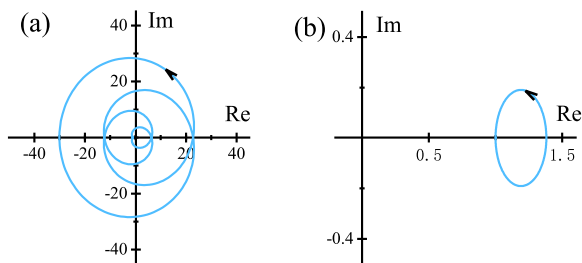


FIG. 3. (a) The Φ dependence of $\det H(\Phi)/|\det H(0)|$ in the complex plane for (a) $W = 3.5$ and (b) $W = 6.5$. The lattice size is $L = 10$ and $\phi = \pi/6$.

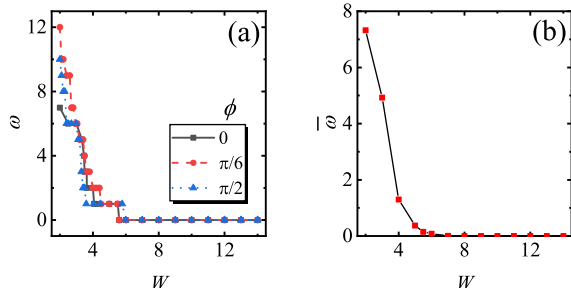


FIG. 4. (a) The W dependence of winding number ω with $\phi = 0, \pi/6$ and $\pi/2$, (b) and the W dependence of averaged winding number $\bar{\omega}$. The lattice size is $L = 10$.

in different universality class for the disorder and quasi-periodic system.

B. Topological phase transition

Different from the Hermitian systems, to study the topological phases of non-Hermitian systems, not only the ground state but also the full complex spectra should be taken into account^{45,46}. Therefore, a natural topological object arising from the complex energy plane is the winding number, that is, a loop constituted by eigenenergies which encircles a prescribed base point. The winding number is topologically stable and changes its value only when curve is crossing the base point. Recently, the winding number has been defined to study the topological phase for non-Hermitian systems in single particle picture without interactions^{45,46}. Generalizing the idea of defining the winding number to our interacting non-Hermitian systems, a parameter Φ is introduced through a gauge transformation $\hat{b}_j \rightarrow e^{i\frac{\Phi}{L}j}\hat{b}_j$ and $\hat{b}_j^\dagger \rightarrow e^{-i\frac{\Phi}{L}j}\hat{b}_j^\dagger$, which can be viewed as a magnetic flux Φ through non-Hermitian ring with length L is applied. The Hamiltonian becomes

$$H(\Phi) = \sum_{j=1}^L [-J(e^{-g}e^{-i\frac{\Phi}{L}}\hat{b}_{j+1}^\dagger\hat{b}_j + e^g e^{i\frac{\Phi}{L}}\hat{b}_j^\dagger\hat{b}_{j+1}) + U\hat{n}_j\hat{n}_{j+1} + W_i\hat{n}_j], \quad (4)$$

and subsequently the winding number is defined as⁴⁵

$$\omega = \int_0^{2\pi} \frac{d\Phi}{2\pi i} \partial_\Phi \ln \det\{H(\Phi) - E_B\}. \quad (5)$$

Here, E_B is the prescribed basis point which is not an eigenenergy of $H(\Phi)$. Different from the bulk-edge correspondence in the hermitian systems, a positive (negative) winding number ω implies a ω ($-\omega$) independent edge modes localized at the left (right) boundary in the semi-infinite space. As demonstrated in Ref.⁴⁵, the winding number does not depend on E_B . The basis point is chosen as $E_B = 0$ in the calculation, so that the loop ensures the coexistence of the $\text{Im}E < 0$ and $\text{Im}E > 0$.

It is not convenient to directly show the loop for the many-body systems, alternatively, we here use the Φ dependence of $\det H(\Phi)/|\det H(0)|$ to illustrate the loop winding around the base point⁵⁹. During the variation of Φ from 0 to 2π , $\det H(\Phi)/|\det H(0)|$ draws a closed loop in the complex plane, and if the loop winds around the origin m times, the winding number is $\pm m$ ($+$ means the counterclockwise winding, while $-$ means the clockwise winding). In Fig. 3, the Φ dependence of $\det H(\Phi)/|\det H(0)|$ with different W for $L = 10$ are plotted, and the phase is chosen as $\phi = \pi/6$. As seen in Fig. 3 (a), $\det H(\Phi)/|\det H(0)|$ draws a closed curve with surrounding origin four times in the complex plane for $W = 3.5$, while $\det H(\Phi)/|\det H(0)|$ draws a closed curve without surrounding the origin for $W = 6.5$ shown in Fig. 3 (b). It gives that $\omega = 4$ for $W = 3.5$ and $\omega = 0$ for $W = 6.5$.

Since the irrational period breaks the translational invariance, the energy spectra changes with ϕ . Therefore, for a specific W the winding number ω also changes with the phase ϕ . In Fig. 4 (a), the W dependence of ω with different ϕ for $L = 10$ are plotted. Although ϕ induces some differences for these curves, some behaviors are in common. On the one hand, ω decreases with W , which is different from the single particle non-Hermitian system. For the single particle non-Hermitian system, the winding number is found as $\omega = \pm 1$ for the topological phase, which means the many-body non-Hermitian have more complicated topological phases. On the other hand, different curves show that a transition from topological phases with $\omega > 0$ to the trivial phase ($\omega = 0$) appears around $W = 7$. The averaged winding number $\bar{\omega}$ is plotted in Fig. 4 (b), and it is shown that the topological phase transition point is around $W_C^T = 7$.

It should be noted that the topological transition is not equal to the disappearance of the imaginary parts of eigenenergies, although the imaginary parts of eigenenergies are necessary to construct a close loop in the energy plane. The topological phase transition gives another viewpoint on the MBL energy spectra complemented to the complex-real energies transition. This winding number, defined in the complex plane by the gauge transformation, serves as a collective indicator of the energies being complex or real of the original Hamiltonian.

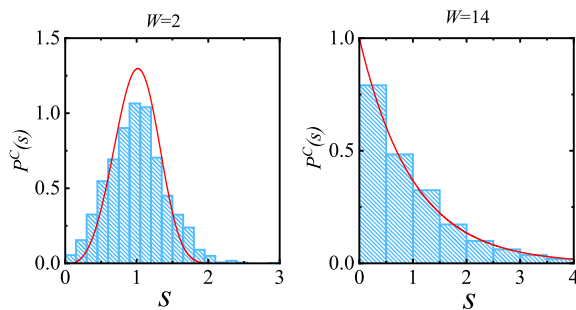


FIG. 5. (a) The nearest-level-spacing distribution (unfolded) for $W = 2$ (left) and $W = 14$ (right). The lattice size is 16, and $\phi = \pi/4$.

C. MBL phase transition

To characterize the MBL in the non-Hermitian systems, the nearest-level-spacing distribution of eigenenergies has been generalized from the Hermitian systems³². On the complex plane, the nearest-level spacings for an eigenenergy E_a (before unfolding) is defined as the minimum distance of $|E_a - E_b|$. For the delocalization phase, it has been demonstrated that the statistics of the nearest-level-spacing obeys a Ginibre distribution $P_{Gin}^c(s) = cp(cs)$, where

$$p(s) = \lim_{N \rightarrow \infty} \left[\prod_{n=1}^{N-1} e_n(s^2) e^{-s^2} \right] \sum_{i=1}^{N-1} \frac{2s^{2n+1}}{n! e_n(s^2)}, \quad (6)$$

with $e_n(x) = \sum_{m=0}^n \frac{x^m}{m!}$ and $c = \int_0^\infty sp(s)ds = 1.1429$ ^{60,61}. Since the MBL tends to suppress the imaginary parts of the complex eigenenergies, these eigenenergies are almost real for the many-body localization state, and the nearest-level-spacing distribution becomes the Poissonian as $P_{Po}^R(s) = e^{-s}$. By taking the eigenenergies lying within $\pm 10\%$ of the real and imaginary parts from the middle of the spectrum of Eq. (1), the nearest-level-spacing distributions (unfolded) for different W are plotted in Fig. 5. It is shown that for $W = 2$ the distribution is a Ginibre distribution and the distribution is a Poisson distribution for $W = 14$. These results demonstrate that the non-Hermitian quasi-crystal also has an MBL phase transition with the increase of W .

Based on the response of the system's eigenstates to a local perturbation, a dimensionless parameter G has been introduced to detect the MBL phases transition in the Hermitian systems⁶². It is shown that G decrease with system size L in the many-body localization phase and grows with system size L in the delocalization phase for the Hermitian systems, and phase transition point appears when $G(L)$ is independent of L . For non-Hermitian system, since the stability of the eigenstates under perturbations \hat{V} is also important for the complex eigenenergies, $G(L)$ has been extend to study MBL phase transition in non-Hermitian systems³². $G(L)$ for the non-

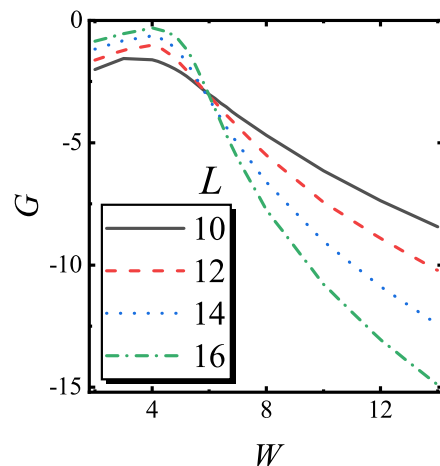


FIG. 6. G as a function of W for $L = 10, 12, 14$ and 16 . The results are obtained by averaging 500 choice of ϕ for $L = 10, 12$ and 14 , and 100 choice of ϕ for $L = 16$.

Hermitian systems is defined as³²

$$G = \ln \frac{\langle \psi_{\alpha+1}^l | \hat{V} | \psi_{\alpha}^r \rangle}{|E'_{\alpha+1} - E'_{\alpha}|}, \quad (7)$$

where $\langle \psi_{\alpha}^l |$ and $|\psi_{\alpha}^r \rangle$ are the left and right eigenvectors of non-Hermitian systems, \hat{V} is a perturbation operator, and $E'_{\alpha} = E_{\alpha} + \langle \psi_{\alpha}^l | \hat{V} | \psi_{\alpha}^r \rangle$ is the modified eigenenergy. Here, the states with E'_{α} stays real are only considered, and the local operator is selected as $\hat{V} = \hat{b}_{i+1}^+ \hat{b}_i$. In Fig. 6, G as a function of W for different L are plotted. It is found that in the many-body delocalized phase the absolute value of G decreases with L , while the absolute value of G grows with L in the MBL phases, and the MBL phase transition occurs at $W_C^{MBL} = 6 \pm 0.2$.

From our numerical calculation, we find that W_C^R , W_C^T and W_C^{MBL} are close, and the slightly difference is attributed to the finite-size effect. Therefore, based on the numerical results, we can conjecture these transition points should coincide in the thermodynamic limit.

D. Effects on the dynamical behaviors

Finally, the effects of the phase transition on the dynamical stability of the non-Hermitian systems are studied. To illustrated this, the time evolution of real part of energy $E^R(t)$ and half-chain entanglement $S(t)$ are studied. $E^R(t)$ is defined as

$$E^R(t) = \text{Re}[\langle \psi^r(t) | \hat{H} | \psi^r(t) \rangle]. \quad (8)$$

Here, $\langle \psi(t)^r |$ is the hermitian conjugate of $|\psi^r(t)\rangle$. As shown in Fig. 7 (a), the time evolution of $E^R(t)$ with different W for $L = 12$ are plotted. It is found that for $W < W_C^R$ and around W_C^R , $E^R(t)$ changes significantly during the evolution since the nonzero imaginary parts

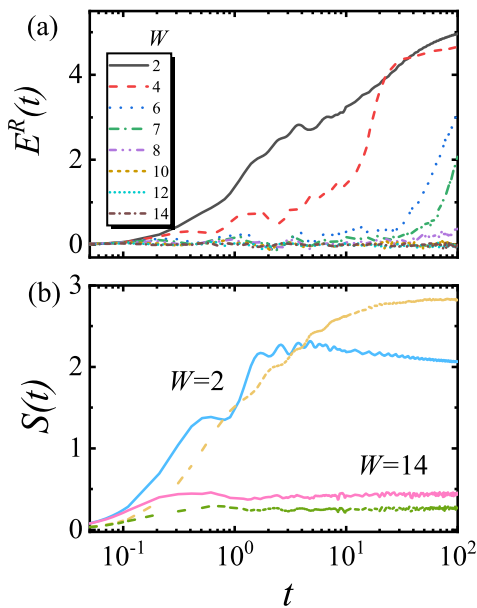


FIG. 7. Time evolution of $E^R(t)$ for $W = 2, 4, 6, 7, 8, 10, 12$ and 14 , (a) and the time evolution of $S(t)$ for $g = 0.5$ (solid lines) and $g = 0$ (dotted lines) (b). The lattice size is $L = 12$, and the initial state is taken as $|\psi_0\rangle = |1010\dots\rangle$.

of the eigenenergies can induce the dynamical instability. For W is much larger than W_C^R , $E^R(t)$ is almost conserved during the evolution, since the eigenvalues are almost real.

The half-chain entanglement $S(t)$ is measured by the von Neumann entropy,

$$S(t) = -\overline{\text{Tr}(\rho(t) \ln \rho(t))}, \quad (9)$$

where $\rho(t) = \text{Tr}_{L/2}[|\psi^r(t)\rangle\langle\psi^r(t)|]/\langle\psi^r(t)|\psi^r(t)\rangle$ is the reduced density matrix of the right eigenstate. The time evolution of $S(t)$ for different W are plotted in Fig. 7(b), and the Hermitian case of $g = 0$ is also shown for a comparison. For $W = 14$, the dynamical behaviors of $S(t)$ for $g = 0.5$ is similar to that $g = 0$, since the eigenvalues are almost real for $g = 0.5$. However, for $W = 2$, $S(t)$ first linearly grow for both values of g , but decrease for $t \simeq 5$

only for $g = 0.5$. In addition, the long-time behavior of the entanglement of the delocalized phase is larger than that of the MBL phase. The reason is that MBL phase still obey the area law rather than the volume law even in the non-Hermitian system⁶³.

IV. SUMMARY

In this paper, we have studied the real-complex transition, topological phase transition and MBL phase transition in a non-Hermitian quasi-periodic system having the time-reversal symmetry. Our numerical results showed that these three types of phase transitions coexist for this model, and in the thermodynamic limit these three transition points should coincide. These results demonstrated that the imaginary parts of the eigenenergies are always suppressed by the MBL, and the MBL phase transition should have a topological nature similar to that of the single particle systems. Moreover, the obtained critical exponent for the real-complex transition is different from that of the disorder system, which means the non-Hermitian many-body disorder system and the many-body quasi-periodic system should belong to different universality class. Finally, we find that the real-complex eigenenergies transition can affects the dynamical stability, but the dynamical entanglement still obey the area law for the MBL phase and volume law for the delocalized phase. Recently, the asymmetry hopping has been realized experimentally in a ultracold atomic system⁴⁵, and the many-body localization in the quasi-periodic system has also been experimentally studied⁴. Therefore, we expect our study can be measured in these experiments.

ACKNOWLEDGMENTS

LJZ is supported by the Natural Science Foundation of Jiangsu Province (Grant No. BK20170309) and National Natural science Foundation of China (Grant No. 11704161).

* guangyaohuang@quanta.org.cn

¹ D. A. Abanin, E. Altman, I. Bloch, and M. Serbyn, *Rev. Mod. Phys.* **91**, 021001 (2019).

² D. A. Abanin and Z. Papić, *Ann. Phys. (Berlin)* **7**, 1700169 (2017).

³ R. Nandkishore and D. A. Huse, *Annu. Rev. Condens. Matter Phys.* **6**, 15-38 (2015).

⁴ M. Rispoli, A. Lukin, R. Schittko, S. Kim, M. Eric Tai, J. Léonard, and M. Greiner, *Nature* **573**, 385-389 (2019).

⁵ T. Kohler, S. Scherg, X. Li, H. P. Lüschien, S. Das Sarma, I. Bloch, and M. Aidelsburger, *Phys. Rev. Lett.* **122**, 170403 (2019).

⁶ A. Morningstar and D. A. Huse, *Phys. Rev. B* **99**, 224205 (2019).

⁷ A. Lukin, M. Rispoli, R. Schittko, M. E. Tai, A. M. Kaufman, S. Choi, V. Khemani, J. Léonard, and M. Greiner, *Science* **364**, 256 (2019).

⁸ D. M. Basko, I. L. Aleiner, and B. L. Altshuler, *Ann. Phys. (NY)* **321**, 1126 (2006).

⁹ M. Žnidarič, T. Prosen and P. Prelovsek, *Phys. Rev. B* **77**, 064426 (2008).

¹⁰ A. Pal and D. A. Huse, *Phys. Rev. B* **82**, 174411 (2010).

¹¹ J. A. Kjäll, J. H. Bardarson, and F. Pollmann, *Phys. Rev. Lett.* **113**, 107204 (2014).

¹² R.-Q. He and Z.-Y. Lu, *Phys. Rev. B* **95**, 054201 (2017).

- ¹³ R. Fan, P. Zhang, H. Shen and H. Zhai, *Sci. Bull.* **62**, 707-711 (2017).
- ¹⁴ I. V. Gornyi, A. D. Mirlin and D. G. Polyakov, *Phys. Rev. Lett.* **95**, 206603 (2005).
- ¹⁵ S. Iyer, V. Oganesyan, G. Refael, and D. A. Huse, *Phys. Rev. B* **87**, 134202 (2013).
- ¹⁶ M. Schreiber, S. S. Hodgman, P. Bordia, H. P. Lüschen, M. H. Fischer, R. Vosk, E. Altman, U. Schneider and I. Bloch, *Science* **349**, 842 (2015).
- ¹⁷ H. P. Lüschen, P. Bordia, S. S. Hodgman, M. Schreiber, S. Sarkar, A. J. Daley, M. H. Fischer, E. Altman, I. Bloch, and U. Schneider, *Phys. Rev. X* **7**, 011034 (2017).
- ¹⁸ F. Setiawan, D.-L. Deng and J. H. Pixley, *Phys. Rev. B* **96**, 104205 (2017).
- ¹⁹ S.-X. Zhang and H. Yao, *Phys. Rev. Lett.* **121**, 206601 (2018).
- ²⁰ V. Khemani, D. N. Sheng, and D. A. Huse, *Phys. Rev. Lett.* **119**, 075702 (2017).
- ²¹ M. Lee, T. R. Look, S. P. Lim, and D. N. Sheng, *Phys. Rev. B* **96**, 075146 (2017).
- ²² N. Macé, N. Laflorencie, and F. Alet, *SciPost Phys.* **6**, 050 (2019).
- ²³ F. Weiner, F. Evers, and S. Bera, *Phys. Rev. B* **100**, 104204 (2019).
- ²⁴ S. Xu, X. Li, Y.-T. Hsu, B. Swingle, and S. Das Sarma, *Phys. Rev. Research* **1**, 032039 (2019).
- ²⁵ V. K. Varma and M. Žnidarič, *Phys. Rev. B* **100**, 085105 (2019).
- ²⁶ H. P. Lüschen, P. Bordia, S. Scherg, F. Alet, E. Altman, U. Schneider, and I. Bloch, *Phys. Rev. Lett.* **119**, 260401 (2017).
- ²⁷ H. Zhao, F. Mintert, and J. Knolle, *Phys. Rev. B* **100**, 134302 (2019).
- ²⁸ E. V. H. Doggen and A. D. Mirlin, *Phys. Rev. B* **100**, 104203 (2019).
- ²⁹ H. Yao, H. Khoudli, L. Bresque and L. Sanchez-Palencia, *Phys. Rev. Lett.* **123**, 070405 (2019).
- ³⁰ V. Goblot, A. Štrkalj, N. Pernet, J. L. Lado, C. Dorow, A. Lemaître, L. Le Gratiet, A. Harouri, I. Sagnes, S. Ravets, A. Amo, J. Bloch, and O. Zilberberg, *Nat. Phys.* **10.1038/s41567-020-0908-7**, (2020).
- ³¹ T. Cookmeyer, J. Motruk, and J. E. Moore, *Phys. Rev. B* **101**, 174203 (2020).
- ³² R. Hamazaki, K. Kawabata, and M. Ueda, *Phys. Rev. Lett.* **123**, 090603 (2019).
- ³³ E. Levi, M. Heyl, I. Lesanovsky, and J. P. Garrahan, *Phys. Rev. Lett.* **116**, 237203 (2016).
- ³⁴ M. V. Medvedyeva, T. Prosen, and M. Žnidarič, *Phys. Rev. B* **93**, 094205 (2016).
- ³⁵ S. Mu, C. H. Lee, L. Li, and J. Gong, arXiv: 1911.00023 (2019).
- ³⁶ S. Heußen, C. D. White, and G. Refael, arXiv: 2003.09430 (2020).
- ³⁷ R. El-Ganainy, K. G. Makris, M. Khajavikhan, Z. H. Muslimani, S. Rotter, and D. N. Christodoulides, *Nat. Phys.* **14**, 11 (2018).
- ³⁸ X. Ni, D. Smirnova, A. Poddubny, D. Leykam, Y. Chong, and A. B. Khanikaev, *Phys. Rev. B* **98**, 165129 (2018).
- ³⁹ S. Malzard, C. Poli, and H. Schomerus, *Phys. Rev. Lett.* **115**, 200402 (2015).
- ⁴⁰ L.-J. Zhai, H.-Y. Wang, and G.-Y. Huang, *Entropy* **21**, 836 (2019).
- ⁴¹ J. M. Zeuner, M. C. Rechtsman, Y. Plotnik, Y. Lumer, S. Nolte, M. S. Rudner, M. Segev and A. Szameit, *Phys. Rev. Lett.* **115**, 040402 (2015).
- ⁴² H. Shen, B. Zhen and L. Fu, *Phys. Rev. Lett.* **120**, 146402 (2018).
- ⁴³ D. Leykam, K. Y. Bliokh, C. Huang, Y. D. Chong, and F. Nori, *Phys. Rev. Lett.* **118**, 040401 (2017).
- ⁴⁴ K. Kawabata, K. Shiozaki, M. Ueda, and M. Sato, *Phys. Rev. X* **9**, 041015 (2019).
- ⁴⁵ Z. Gong, Y. Ashida, K. Kawabata, K. Takasan, S. Higashikawa, and M. Ueda, *Phys. Rev. X* **8**, 031079 (2018).
- ⁴⁶ S. Longhi, *Phys. Rev. Lett.* **122**, 237601 (2019).
- ⁴⁷ S. Longhi, *Opt. Lett.* **44**, 1190 (2019).
- ⁴⁸ T. Liu, Y.-R. Zhang, Q. Ai, Z. Gong, K. Kawabata, M. Ueda and F. Nori, *Phys. Rev. Lett.* **122**, 076801 (2019).
- ⁴⁹ D.-W. Zhang, L.-Z. Tang, L.-J. Lang, H. Yan, and S.-L. Zhu, *Sci. China Phys. Mech. Astron.* **63**, 267062 (2020).
- ⁵⁰ Q.-B. Zeng, Y.-B. Yang and Y. Xu, *Phys. Rev. B* **101**, 020201(R) (2020).
- ⁵¹ C.-K. Chiu, J. C. Y. Teo, A. P. Schnyder and S. Ryu, *Rev. Mod. Phys.* **88**, 035005 (2016).
- ⁵² M. F. Lapa, J. C. Y. Teo and T. L. Hughes, *Phys. Rev. B* **93**, 115131 (2016).
- ⁵³ J. Maciejko, X.-L. Qi, A. Karch and S.-C. Zhang, *Phys. Rev. Lett.* **105**, 246809 (2010).
- ⁵⁴ D. A. Huse, R. Nandkishore, V. Oganesyan, A. Pal and S. L. Sondhi, *Phys. Rev. B* **88**, 014206 (2013).
- ⁵⁵ A. Chandran, V. Khemani, C. R. Laumann and S. L. Sondhi, *Phys. Rev. B* **89**, 144201 (2014).
- ⁵⁶ Y. Kuno, *Phys. Rev. Research* **1**, 032026 (2019).
- ⁵⁷ T. Orito, Y. Kuno and I. Ichinose, *Phys. Rev. B* **100**, 214202 (2019).
- ⁵⁸ L.-J. Zhai and S. Yin, arXiv: 1909.09558 (2019).
- ⁵⁹ M. Arikawa, I. Maruyama and Y. Hatsugai, *Phys. Rev. B* **82**, 073105 (2010).
- ⁶⁰ H. Markum, R. Pullirsch and T. Wettig, *Phys. Rev. Lett.* **83**, 484-487 (1999).
- ⁶¹ F. Haake, *Quantum signatures of chaos* (Springer Science Z & Business Media, New Yorkm 2010), Vol.54.
- ⁶² M. Serbyn, Z. Papić and D. A. Abanin, *Phys. Rev. X* **5**, 041047 (2015).
- ⁶³ B. Bauer and C. Nayak, *J. Stat. Mech. Theroy E*. P09005 (2013).